Drug Release from Self-Assembled Inorganic−Organic Hybrid Gels and Gated Porosity Detected by Positron Annihilation Lifetime Spectroscopy

Ansgar Bögershausen,[†] Steven J. Pas,[†] Anita J. Hill,[‡] and Hubert Koller*[,†]

Institute of Physical Chemistry, University of Münster, Corrensstrasse 36, 48149 Münster, Germany, CSIRO Manufacturing and Infrastructure Technology, Victoria, Australia, and School of Chemistry, Monash University, Clayton Victoria, Australia

Received August 18, 2005. Revised Manuscript Received November 23, 2005

Self-assembled silica and hybrid organo−silica sol−gel materials have been prepared in the presence of the pharmaceutically active guest molecule Persantin. The dissolution of the drug molecule and the matrix porosities are related to the synthesis parameters, compositions, and pH values. Whereas larger pores and faster release times are observed at weakly acidic sol−gel reactions (pH 5.6), more dense materials and slower drug-release kinetics are found at values down to pH 2−3. It is shown that organically functionalized host gels can control drug release, depending on the organic functionality. All self-assembled systems show controlled-release profiles compared to the direct-release profile for impregnated silica. Gels with acetoxypropyl-group functionalization show faster release kinetics with an increasing number density of these organic moieties, whereas hybrid gels functionalized with an increasing number of methyl, propyl, phenyl, or benzyl groups inhibit release. Positron annihilation lifetime spectroscopy shows a bimodal pore system for gels prepared at weakly acidic pH values. Only the larger pores are accessible to N_2 adsorption for inorganic silica gels or hybrid gels with methyl or propyl groups. N_2 adsorption for hybrid gels with acetoxypropyl groups is prevented by the organic side chains that gate the pores.

Introduction

Molecular imprinting and the structure direction of nano- or mesoporous solids cover a wide range of materials with applications in catalysis, separation, and sensors, or as hosts for quantum-sized clusters for optics and electronics.[1−3] The generation of ordered porous materials also entails the structure direction of the void space by organic moieties that are usually encapsulated in the matrix during synthesis. To make the pore system accessible, for example, for catalytic applications, we have to remove the structure-directing agent by either calcination in air or extraction. Further interest in the fabrication of porous materials encompasses the generation of drug-release systems. The most common materials are organic hydrogels or polymers.[4−8] An alternative approach to polymeric systems involves embedding the drug molecule in ordered mesoporous systems, for example, mesoporous silica, MCM-41,[9] or intercalation of the drug in layered aluminosilicates such as double-layer hydroxides and clays.[10] A recent study by Chang et al. uses swollen, thermoresponsive nanocomposites.[11] In most cases, the porous matrix is made by a structure-directing agent or imprint molecule that differs from the drug to be released, and the latter has to be adsorbed in the empty pore space in a second step. The purpose of this study is the generation of inorganic−organic hybrid sol−gel systems, with pores that are imprinted or filled by the drug itself in the sol−gel reaction. The focus is the investigation of the structure-directing ability of a drug molecule by choosing appropriate precursors for the sol−gel process, the characterization of the drug-release rate, and the porosity of the extracted inorganic−organic matrices. We present a new drug-carrier system that consists of silica hybrid gels having organic side groups. A major difference from existing formulations is that the matrix is generated in the presence of the drug molecule in a self-assembling process. It will be shown that such an amorphous drug-carrier system with organic side groups provides the ability to tailor the drug-release kinetics by controlling pore size and accessibility. Special attention will be given to the pore structure after drug release.

The critical role of pore architecture (size and accessibility) in the tailored drug release is revealed by nitrogen adsorption and positron annihilation lifetime spectroscopy (PALS).

* To whom correspondence should be addressed. E-mail: hubert.koller@uni-muenster.de. Phone: 49 251 8323448. Fax: 49 251 8323409.

[†] University of Münster.

[‡] CSIRO Manufacturing and Infrastructure Technology and Monash University.

(1) Davis, M. E.; Katz, A.; Ahmad, W. R. *Chem. Mater.* **1996**, *8*, 1820.
(2) Díaz-García, M. E.; Badía Laíño, R. *Microchim. Acta* **2005**, *149*, 19.
(3) Asanuma, H.; Hishiya, T.; Komiyama, M. *Adv. Mater.* **2000**, *12*, 1019.
(4) Byrne, M. E.; Park, K.; Peppas, N. A. *Adv. Drug Delivery Rev.* **2002**, *54*, 149.
(5) Malmsten, M. *Surfactants and Polymers in Drug Delivery*; Marcel Dekker: New York, 2002.
(6) Unger, K.; Rupprecht, H.; Valentin, B.; Kircher, W. *Drug Dev. Ind. Pharm.* **1983**, *9*, 69.
(7) Kortesuo, P.; Ahola, M.; Kangas, M.; Leino, T.; Laakso, S.; Vuorilehto, L.; Yli-Urop, A.; Kiesvaara, J.; Marvola, M. *J. Controlled Release* **2001**, *76*, 227.
(8) Böttcher, H.; Slowik, P.; Süss, W. *J. Sol−Gel Sci. Technol.* **1998**, *13*, 277.
(9) Vallet-Regi, M.; Rámila, A.; del Real, R. P.; Pérez-Pariente, J. *Chem. Mater.* **2001,** *13*, 308.
(10) Bringley, J. F.; Liebert, N. B. *J. Dispersion Sci. Technol.* **2003**, *24*, 589.
(11) Chang, J. H.; Chang, H. S.; Kim, B. J.; Shin, Y.; Exarhos, G. J.; Kim, K. J. *Adv. Mater.* **2005**, *17*, 634.

10.1021/cm051859o CCC: $33.50
Published on Web 01/06/2006

PALS provides information on the pore characteristics of materials.[12,13] Positrons (e^+) are the antiparticles of electrons (e^-). In condensed matter, the positrons annihilate with electrons in the regions of the sample that are probed by the positron wave function. The positron lifetime is inversely proportional to the electron density in these regions. The discovery[12] in 1960 that *o*-positronium, oPs (e^+e^-), can become localized in pores has led to the development of PALS as a method for studying the size distribution and dynamics of pores.

The oPs atom is a semistable atom composed of a positron and an electron with parallel spins. In a vacuum, oPs decays by self-annihilation in 140 ns. In an organic−inorganic gel, the high electron density makes it most probable that the oPs will annihilate with an electron (from one of the gel atoms) with opposite spin (pickoff annihilation) that reduces the oPs lifetime to a few nanoseconds. Before annihilation, the oPs will localize in a void because of the repulsion between the oPs electron and the electrons in the surrounding atoms or molecules. The oPs lifetime is a function of the exchange interaction between the oPs electron and the electrons bound to the molecules forming the void. As the void gets larger, the exchange probability (probability of wave function overlap) decreases, and the oPs lifetime increases.

The PALS technique relies on the ability to inject positrons into the gel and to measure the positron−electron annihilation rates. The positron lifetime is the inverse of the annihilation rate. The data are collected in the form of a timing histogram with distinct timing intervals for the positron annihilation lifetimes. The short lifetime (100−200 ps) is attributed to the self-annihilation of *p*-positronium (pPs), formed when a positron and electron of antiparallel spin combine; the intermediate lifetime (300−600 ps) is attributed to the annihilation of free and trapped positrons; the longest lifetime (1−20 ns) is attributed to oPs pickoff annihilation. For oPs lifetimes greater than 20 ns, the decay mechanism is a combination of pickoff and self-annihilation.[14] In many materials, there are two oPs components that exhibit distinct lifetimes longer than 1 ns. In such materials, these two oPs components are often interpreted in terms of a bimodal distribution of pore volumes (e.g., smaller cavities and larger voids found in zirconia−silica sol−gels[15]).

The three (or sometimes four) lifetimes can be extracted by a nonlinear least-squares fit of a weighted sum of discrete exponentials according to

$$N(t) = \sum_{i=1}^{n} \frac{I_i}{\tau_i} \exp\left(-\frac{t}{\tau_i}\right)$$

Here, τ_i denotes the mean lifetime of the positron state i, I_i is the relative intensity of the lifetime component, and n is the number of positron states. The oPs pickoff lifetimes, τ_{oPs}, can be related to a void radius R, for R up to 1 nm, using a semiempirical model[16,17] in which the oPs localizes and annihilates in an infinite spherical square well potential with a finite electron-layer thickness. However, for $R > 1$ nm, the oPs can no longer be represented by a standing wave function in a potential well. For these larger pores, it is approximated that the oPs annihilates either in a surface state on the pore wall or via self-annihilation in the center of the pore as if in a vacuum (i.e., without the availability of pickoff electrons from the pore wall). A modified semiempirical model is used for pore sizes with radii from 1 to 4 nm.[13]

The positrons are implanted into the gel with a range of energies, leading to penetration depths of a few micrometers to 1 mm. This implantation process enables oPs to find voids that do not need to be connected to the surface, unlike surface methods such as N_2 adsorption. Both internal and external pores are accessible to oPs, and a range of pore sizes can be probed by this method, from the size of the oPs (van der Waals radius of 0.13 nm) up to a radius of 4 nm.

Scheme 1. Persantin (PS)

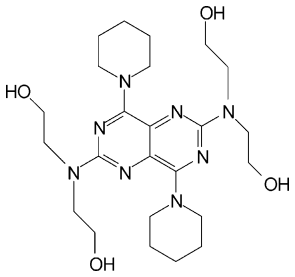

Experimental Section

N,*N*′-(4,8-dipiperidino-pyrimido[5,4-d]pyrimidin-2,6-diyl)bis-(2,2′-iminodiethanol), or Persantin (PS), Scheme 1, is a yellow crystalline powder and was used as obtained from Boehringer Ingelheim Pharma GmbH & Co KG company.

It is a coronary vasodilator and is also used to prevent platelet aggregation after heart valve disease.[18] It was incorporated in situ into silica hybrid gels during sol−gel syntheses from tetraethyl orthosilicate (TEOS, Q monomer), and a second T monomer precursor, R−Si(OEt)$_3$ or R−Si(OMe)$_3$.

Gels without T Monomer. The first parameter that was varied was the pH value. In a typical two-step sol−gel synthesis, 0.9 g of PS was dissolved in a mixture of ethanol and 0.5 M HCl; this solution was slowly added to TEOS. After the solution was stirred for 1 h, the pH was varied by adding concentrated HCl or 0.5 M NH_3. The obtained solution was again stirred for 1 h and then subjected to further sol−gel reaction at 323 K in an open system to allow solvent evaporation. The final relative molar ratios and pH values of the sol formulations are given in Table 1. For comparison, two materials are prepared in which PS was not incorporated into the gels in situ. The first material is a physical mixture of a TEOS-derived gel (pH 5, TEOS:EtOH:HCl:H_2O = 1:5:0.06:7.2) and pure crystalline PS. The second material was a physically impregnated commercial silica (Cab-o-Sil M5, Fluka). The silica was stirred in a solution of 1500 mg of PS in 20 mL of chloroform for 24 h. After that, the material was dried at 323 K to remove the solvent.

(12) Brandt, W.; Berko, S.; Walker, W. W. *Phys. Rev.* **1960**, *120*, 1289.
(13) Shrader, D. M.; Jean, Y. C. *Positron and Positronium Chemistry*; Elsevier: Amsterdam, 1988.
(14) Ito, K.; Nakanishi, H.; Ujihira, Y. *J. Phys. Chem. B* **1999**, *103*, 4555.
(15) Misheva, M.; Djourelov, N.; Margaca, F. M. A.; Miranda Salvado, I. M. *J. Non-Cryst. Solids* **2000**, *272*, 209.
(16) Tao, S. *J. Chem. Phys.* **1972**, *56*, 5499.
(17) Eldrup, M.; Lightbody, D.; Sherwood, J. N. *Chem. Phys.* **1981**, *63*, 51.
(18) Mutschler, E. *Arzneimittelwirkungen*; Wissenschaftliche Verlagsgesellschaft: Stuttgart, Germany, 1997.

Table 1. Total Molar Ratios, pH Values before Gel Formation, and Gelation Times[a]

Relative Molar Ratios with only Q Monomer

gel no.	gel	TEOS	EtOH	HCl	H_2O	PS	pH	t_{gel} (days)
1	(TPS1)	1	4.0	0.046	5.16	0.041	0.8	24
2	(TPS2)	1	4.0	0.046	5.16	0.041	2.5	24
3	(TPS3)	1	4.0	0.046	5.16	0.041	3.8	24
4	(TPS4)	1	4.0	0.046	5.16	0.041	4.5	24
5	(TPS5)	1	4.0	0.046	5.16	0.041	5.6	24

Relative Molar Ratios of Gels with T Monomer PTS

gel no.	gel	TEOS	PTS	EtOH	HCl	H_2O	PS	pH	t_{gel} (days)
6	(PTSPS05)	1	0.2	4.80	0.043	4.67	0.050	5	<3
7	(PTSPS06)	1	0.25	4.80	0.045	4.97	0.050	5	<5
8	(PTSPS07)	1	0.33	4.80	0.046	5.13	0.050	5	<6
9	(PTSPS10)	1	0.1	1.18	0.041	4.60	0.050	5	0.5
10	(PTSPS11)	1	0.2	1.29	0.045	5.00	0.053	5	3
11	(PTSPS12)	1	0.25	1.25	0.044	4.84	0.052	5	6
12	(PTSPS13)	1	0.33	1.33	0.047	5.17	0.055	5	14
13	(PT5-1)	1	0.2	1.20	0.042	4.66	0.050	1−2	<1

Relative Molar Ratios of Gels with T Monomer MTS

gel no.	gel	TEOS	MTS	EtOH	HCl	H_2O	PS	pH	t_{gel} (days)
14	(MTSPS02)	1	1	5.40	0.090	10.0	0.080	4−5	5
15	(MTSPS03)	1	0.2	4.80	0.056	6.22	0.050	4−5	3
16	(MTSPS04)	1	0.33	5.34	0.062	6.92	0.056	4−5	4−5
17	(MTSPS05)	1	0.1	4.38	0.051	5.67	0.046	5	0.5
18	(MTSPS07)	1	0.25	4.97	0.058	6.45	0.052	5	4
19	(MTSPS08)	1	0.5	5.97	0.070	7.73	0.062	5	6
20	(MTSPS09)	1	1	7.95	0.093	10.3	0.083	5	14

Relative Molar Ratios of Gels with T Monomer ATS

gel no.	gel	TEOS	ATS	EtOH	HCl	H_2O	PS	pH	t_{gel} (days)
21	(AT7-1)	1	0.14	1.14	0.053	5.90	0.047	1.5	<0.5
22	(AT4-1)	1	0.25	1.24	0.058	6.44	0.052	1.5	<0.5
23	(AT2-1)	1	0.50	1.50	0.070	7.77	0.062	1.5	<0.5
24	(ATSPS40-01b)	1	0.14	1.14	0.053	12.00	0.053	4.5	<0.5
25	(ATSPS40-02b)	1	0.25	1.24	0.058	13.22	0.061	4.5	<0.5
26	(ATSPS40-03b)	1	0.50	1.50	0.070	15.93	0.073	4.5	<0.5

[a] Note that different reaction temperatures apply (see text).

Gels with T Monomer PTS. A mixture of the solution of PS, ethanol, and 0.5 M HCl and the solution of the two precursors TEOS and propyltriethoxysilane, PTS, with a pH of 1.6, was prepared, covered, and stirred. Samples 6−8 were kept on the stirrer for 12 h for hydrolysis. NH_3 (1.0 M) was then added until the pH reached 5. Samples 9−13 were stirred for 3 days, and then 0.5 M NH_3 was slowly added until the pH reached 5, except for gel 13, which was kept at pH 1−2. The clear solutions were stirred for 1 h; they were then reacted at room temperature and dried at 323 K until the mass did not change further. Sample 13 was stirred for 1 h at room temperature and then reacted at 323 K.

Gels with T Monomer MTS. These gels were prepared using a procedure similar to that for the gels without a T monomer. A mixture of the solution of PS, ethanol, and 0.5 M HCl and the solution of the two precursors TEOS and methyltriethoxysilane, MTS, with a pH of 1.5, was covered and stirred for hydrolysis. The solutions of gels 14−16 were stirred for 12 h, and 0.5 M NH_3 was then added until the pH reached 4−5. The clear solutions were stirred for 1 h; they were then reacted at room temperature and dried at 323 K until the mass did not change further. The solutions of gels 17−20 were stirred for 3 days, and 0.5 M NH_3 was then added until the pH reached 5. The clear solutions were stirred for 1 h; they were then reacted at room temperature and dried at 323 K.

Gels with T Monomer ATS. The solutions were prepared in the same way as before, but acetoxypropyltrimethoxysilane, ATS, was used. The first three gels, 21−23, were prepared in a one-step process without increasing the pH. The clear and homogeneous sols with a pH of 1.5 were stirred at room temperature for 3 h and then reacted at 323 K until dry xerogels had formed.

The second set of gels with ATS, 24−26, were prepared in a two-step process. The solutions were stirred for 12 h before slowly adding 0.5 M NH_3 until the final pH value was reached; the solutions were stirred for 1 h and then reacted at 323 K until dry xerogels had formed.

All gels were treated in a ballmill for 2 min at 200 rpm to obtain a similar particle-size distribution, which was measured by light scattering on selected batches.

Instrumental. The dissolution profiles of PS from silica particles were studied using the U.S.P. 24 dissolution apparatus II (paddle method, VanKel VK7010). A 900 mL solution of 0.1 wt % HCl and 0.05 wt % sodium dodecyl sulfate was used as a dissolution medium. The rotation speed was 100 rpm, and the temperature was 37 °C. The absorbance values of the dissolution samples were measured with an UV−vis spectrophotometer (Cary 100, Varian).

Nitrogen adsorption experiments were carried out on a Micromeritics ASAP 2010. The samples were dehydrated for 8 h under vacuum at 373 K before adsorption. ^{29}Si MAS NMR spectra were acquired on a Bruker CXP-300 spectrometer without cross-polarization, which allowed us to gain quantitative information about the distribution of building units (Q sites).

The PALS measurements were performed in dry N_2 at ambient temperature using an automated EG&G Ortec fast−fast coincidence system. The timing resolution of the system was 240 ps, determined by using the prompt curve from a ^{60}Co source with the energy windows set to ^{22}Na events. For the PALS experiments, the gel

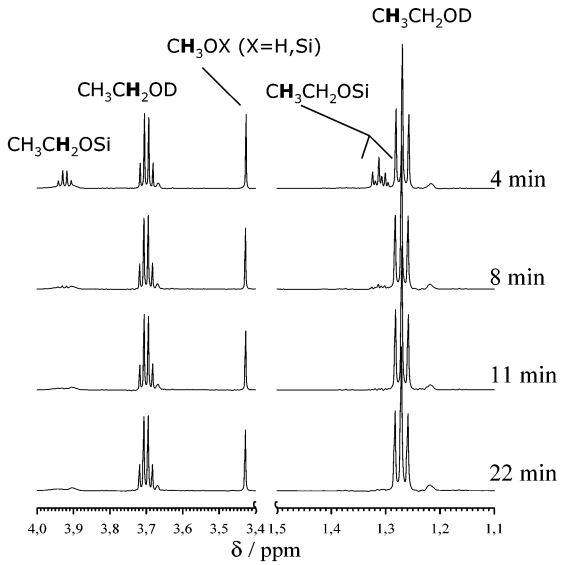

Figure 1. ^{1}H NMR spectra of a representative 4:1 synthesis mixture of TEOS:ATS at different stirring times and pH 1.5.

powders were dried at 50 °C. The powders were packed to a total thickness of 2 mm on either side of the 30 μCi ^{22}Na−Ti foil source. For each sample, 5−10 spectra were collected. The oPs lifetime and intensity values were each averaged to yield the mean values reported here. Each spectrum consisted of approximately 1 million integrated counts.

Results and Discussion

Hydrolysis and Condensation Kinetics. A key requirement for the formation of hybrid gels and the avoidance of phase separation is that the hydrolysis and condensation kinetics of all gel precursors are similar. The similar rates will then ensure that entropic driving forces prevail, achieving a high dispersion of the different building units. To gain a deeper insight into the kinetics, ^{1}H and ^{29}Si NMR spectroscopy have been employed in situ on the reaction solutions of tetraethyl orthosilicate, TEOS, and acetoxypropyltrimethoxysilane, ATS.

Figure 1 shows the ^{1}H NMR spectra of the TEOS−ATS reaction mixture in an acidic solution under the hydrolysis conditions that are applied to all reactions. The mixture was made using the same procedure and with the same composition as those of gel 22, but ethanol-d_6, DCl, and D_2O were used. For clarity, only the ethyl and methyl group region is shown, in which CH_3CH_2OX or CH_3OX groups are either in the precursor molecules (X = Si) or in the alcohol that is formed in the hydrolysis or condensation reactions (X = H). The pH value of the reaction mixture was 1.5. The ethanol peaks are shown as a quartet at 3.70 ppm and as a triplet at 1.27 ppm. The quartet at 3.93 ppm is due to CH_2 groups in TEOS, and the CH_3 groups show two separate triplets at ca. 1.31 ppm. The occurrence of the two triplets is assumed to be due to TEOS at different hydrolyzation stages. The methyl groups of ATS and methanol yield the same peak at 3.43 ppm. The first spectrum, taken 4 min after mixing the components, already shows that most of the ethoxy groups have been hydrolyzed; after 8 min, this reaction is complete. All sol−gel preparations involved a hydrolysis at an acidic pH value for at least 60 min; thus, it is safe to conclude that hydrolysis of TEOS has been completed. No conclusion regarding hydrolysis of ATS can be made from ^{1}H NMR.

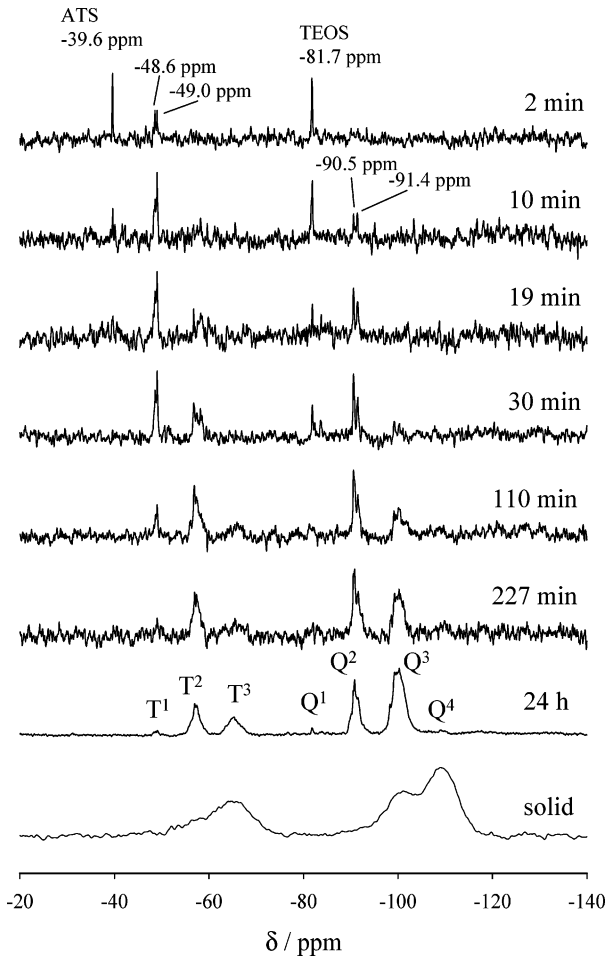

Figure 2. ^{29}Si NMR spectra of the same mixture as that in Figure 1.

The condensation of the precursors is observed by ^{29}Si NMR spectroscopy of the reaction mixture (Figure 2). The established nomenclature with T and Q groups is adopted here; T stands for R−Si(OX)$_3$ and Q for Si(OX)$_4$ (X = H, Si, R′). The precursor monomers, ATS and TEOS, yield T^0 and Q^0 single lines at −39.6 and −81.7 ppm, respectively. This assignment was confirmed by ^{29}Si NMR on pure precursor solutions. After 2 min, there are lines at −48.6 and −49.0 ppm in the T^1 region, whereas no lines are observed in the chemical shift region of Q units other than for TEOS. The integrated intensity ratios of the peaks at −39.6 and −81.7 ppm are consistent with the T:Q ratio. After 10 min, lines at −90.5 and −91.4 ppm appear, indicating a condensation to Q^2 units. A signal of silicic acid (Q^0) at ca. −70 ppm was never observed. This indicates that hydrolyzed TEOS undergoes an instant condensation to oligomers. It should be noted that the chemical shift of TEOS at −81.8 ppm is in the same range as that where Q^1 species of dimers or end groups of chains appear.[19] As the reaction proceeds, progress in the condensation can be identified in the ^{29}Si NMR spectra. The composition at 24 h shows a distribution of T^1, T^2, and T^3 as well as Q^1, Q^2, Q^3, and a rather small amount of Q^4 units. The kinetics of the condensation

(19) Brinker, C.; Scherer, G. *Sol−Gel Science: The Physics and Chemistry of Sol−Gel Processing;* Academic Press: New York, 1990.

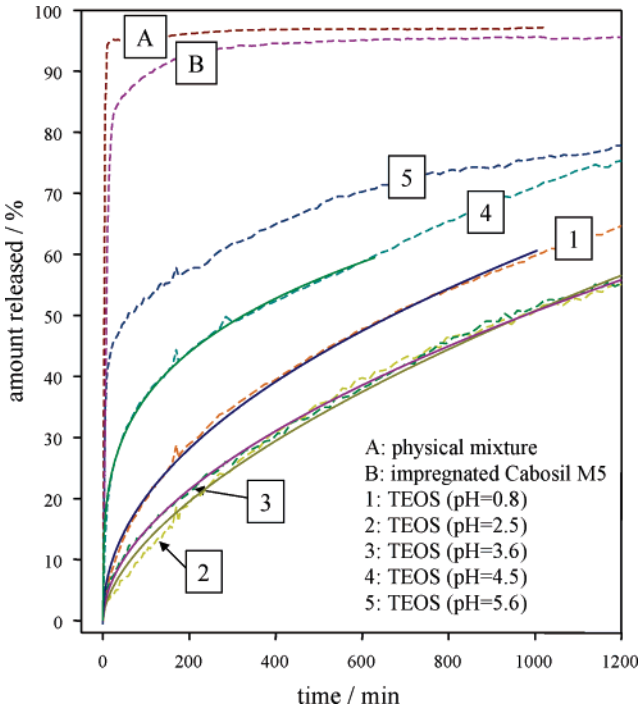

Figure 3. Drug-release experiments of silica gels (cf. Table 1); solid lines are fits (see text).

reactions appears to be slightly faster for the ATS precursor products at early stages of condensation, but only dimeric T^1 groups occur; such small oligomeric groups are soluble in such mixtures and would not cause phase separation. There is a considerable condensation of T and Q units in solution in comparable times. The solution had a homogeneous and clear appearance in the course of these liquid NMR experiments.

The solid gel product has a higher number of connectivities, which is shown by the high number density of T^3 and Q^4 in the ^{29}Si solid-state NMR spectrum (bottom of Figure 2). The T:Q ratio in the solid is consistent with the 1:4 stoichiometry.

It is concluded from ^{1}H and ^{29}Si NMR spectroscopy that ATS and TEOS form a hybrid gel with mixed T and Q units. Hydrolysis is faster than condensation, and both are similar for the two precursors, enabling a controlled-reaction protocol.

Single-Precursor Gels. The first parameter having a possible influence on drug release is the synthesis pH value in the sol−gel process. Therefore, a number of gels with only TEOS as a precursor have been prepared at different pH values, as described in the Experimental Section. For comparison, physical mixtures of Persantin with an unloaded gel made from TEOS as well as Cabosil M5 silica impregnated with Persantin have been investigated in terms of their kinetic drug-release profiles.

Figure 3 shows the relative amounts of Persantin released into a 0.1% HCl (aq) solution from different drug-carrier systems as a function of time. It is obvious that an instant release occurs for the bulk drug in a physical mixture with silica gel as well as from an impregnated commercial Cabosil M5 silica gel (samples A and B in Figure 3, respectively).

The other samples in Figure 3 are silica gels made at different pH values from 5.6 to 0.8 in the presence of the drug. A strong dependence of the release profile on the pH value is observed. Interestingly, a fast initial release occurs for gels which are made at the higher pH values of 5.6 and 4.5. The most acidic system then follows (pH 0.8), and finally the minimum in the release curvature profile occurs for the pH values of 3.6 and 2.5. The release curves have been fitted up to a maximum release of 60% with the following equation[20,21]

$$M/M_0 = kt^n$$

The fitted parameters k and n are listed in Table 2.

Table 2. Kinetic-Release Parameters of Carrier Gels

sample	k	n
1: TEOS, pH 0.8	2.28 ± 0.04	0.475 ± 0.003
2: TEOS, pH 2.5	0.83 ± 0.04	0.594 ± 0.007
3: TEOS, pH 3.6	1.27 ± 0.02	0.534 ± 0.003
4: TEOS, pH 4.5	10.8 ± 0.1	0.264 ± 0.002
5: TEOS, pH 5.6	30.5 ± 0.4	0.120 ± 0.003
9: TEOS:PTS 10:1, pH 5	3.63 ± 0.06	0.330 ± 0.002
10: TEOS:PTS 5:1, pH 5	2.21 ± 0.03	0.346 ± 0.002
12: TEOS:PTS 3:1, pH 5	1.04 ± 0.02	0.363 ± 0.002
13: TEOS:PTS 5:1, pH 1−2	1.47 ± 0.02	0.391 ± 0.002
21: TEOS:ATS 7:1, pH 1.5	0.50 ± 0.02	0.619 ± 0.005
22: TEOS:ATS 5:1, pH 1.5	1.06 ± 0.03	0.546 ± 0.004
23: TEOS:ATS 2:1, pH 1.5	1.49 ± 0.02	0.515 ± 0.002
24: TEOS:ATS 7:1, pH 4.5	6.8 ± 0.1	0.311 ± 0.003
25: TEOS:ATS 5:1, pH 4.5	6.8 ± 0.2	0.342 ± 0.004
26: TEOS:ATS 2:1, pH 4.5	8.9 ± 0.2	0.341 ± 0.005

The diffusion exponent, n, contains information about the diffusion mechanism. For spherical particles, a value of 0.43 would be expected for Fickian diffusion. Larger values of n originate from anomalous non-Fickian behavior. Smaller values are usually ascribed to a distribution of particle size.[22] Smaller values of n may also arise from an initial burst effect, possibly caused by instant dissolution from external surfaces. The prefactor, k, describes the release and interaction properties of the guest−host system.

Before these results on the release kinetics are further discussed, nitrogen adsorption isotherms and PALS data on the extracted sol−gel materials are also presented. The N_2 adsorption capacity varies considerably and consistently as a function of the synthesis pH value for gels extracted for 960 min (Figure 4).

Whereas the release profile shows a minimum at pH values of 3.6 and 2.5, the adsorption isotherms in Figure 4 show a clear correlation between the total volumes of adsorbed nitrogen and synthesis pH values. It is surprising that gels 1 and 2 in Figure 4 show no adsorption capacity, although they have released an appreciable amount of Persantin after 960 min of extraction (Figure 3). Gels 3 and 4 show an adsorption isotherm that is typical for a microporous system. Gel 5, made at the highest pH value of 5.6, also shows some mesoporous contributions to the adsorption isotherm.

The unexpected adsorption capacities for the most acidic gels were the reason for a deeper study on pore structure using positron annihilation lifetime spectroscopy (PALS). Figure 5 shows the PALS experiments of gels 1 (pH 0.8) and 5 (pH 5.6). The decay curves were analyzed beginning at the peak maximum, using the components as explained

(20) Ritger, P. L.; Peppas, N. A. *J. Controlled Release* **1987**, *5*, 23.
(21) Peppas, N. A. *Pharm. Acta Helv.* **1985**, *60*, 110.
(22) Ritger, P. L.; Peppas, N. A. *J. Controlled Release* **1987**, *5*, 37.

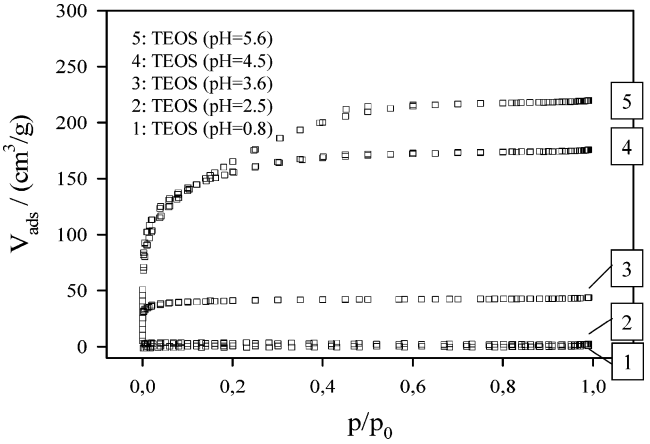

Figure 4. N_2 adsorption isotherms of the extracted gels of Figure 3.

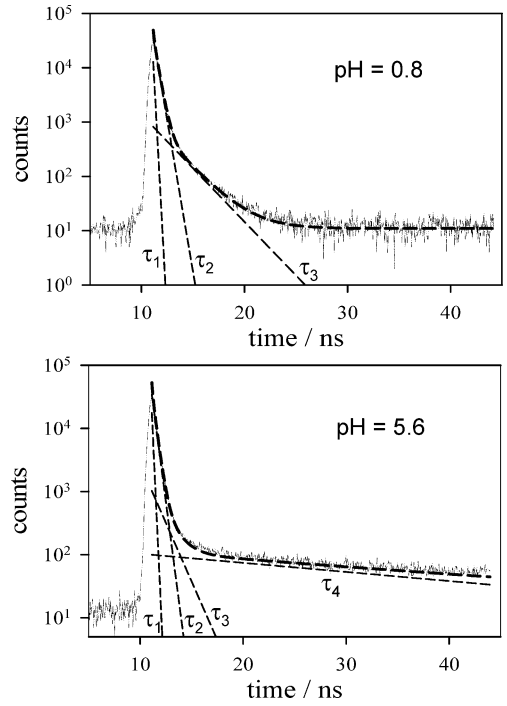

Figure 5. PALS experiment of samples 1 and 5.

Table 3. oPs Lifetimes and Pore Radii for Extracted (960 min) Silica Gels Made from TEOS

sample	$\tau_3 \pm 0.06$	R (nm)	$\tau_4 \pm 0.9$	R (nm)
1: TEOS, pH 0.8	2.17	0.301		
2: TEOS, pH 2.5	2.16	0.300		
3: TEOS, pH 3.6	1.13	0.186	4.9	0.471
4: TEOS, pH 4.5	2.07	0.292	17.1	0.825
5: TEOS, pH 5.6	1.20	0.197	30.3	1.4

in the Introduction. The decay constants τ_1 and τ_2 are attributed to pPs self-annihilation (125 ps) and free and trapped positrons (300−600 ps), respectively, and are not further discussed here. The more acidic gel (pH 0.8) in Figure 5 shows a τ_3 component of 2.17 ns, and the less acidic gel (pH 5.6) shows a τ_3 of 1.2 ns and a τ_4 of 30.3 ns (Table 3). Similar PALS experiments have been performed on the other silica gels after drug release.

It is striking that those gels (1 and 2) that do not show a nitrogen adsorption capacity have only a τ_3 component in the PALS experiment, whereas the other gels also have a τ_4 component. Therefore, Persantin must be extracted from a bimodal pore system. One type of pore is characterized by a shorter oPs lifetime, τ_3, and these smaller pores are inaccessible to nitrogen. The other type of pore gives a longer oPs lifetime, τ_4, and these pores are also observed in the nitrogen adsorption isotherms. An oPs lifetime, τ_3, of 2.16 ns corresponds to a spherical pore diameter of 0.6 nm, according to the Tao−Eldrup equation.[16,17] This value is too small to accommodate a Persantin molecule. Thus, it is very likely that the gel structure shrinks upon drug release, and PALS observes only the residual size of contracted, possibly partially H_2O filled, pores.

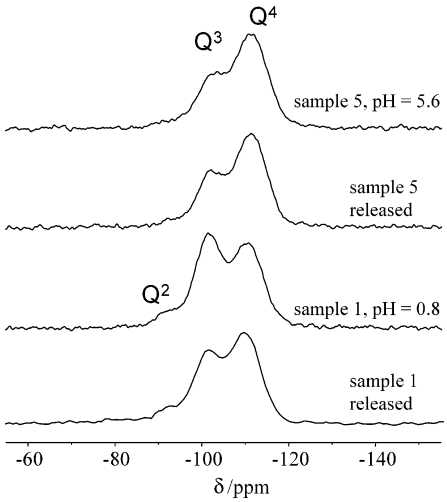

Figure 6. ^{29}Si MAS NMR of samples 1 and 5 before and after drug release.

Summarizing the experimental data on these single-precursor gels, we find the strong pH dependence of both the nitrogen adsorption capacity (Figure 4) and the pore size as measured by PALS; when this result is compared to the drug-release profile, it follows that the gel structure for the low-pH (0.8, 2.5) gels collapses following drug dissolution. From the small pore diameter (0.6 nm on the basis of PALS analysis) of the most acidic gels, it follows that there must be a substantial degree of shrinking of the gels upon drug release, because a void space of this size would not accommodate Persantin. This applies mainly to the small pores in the bimodal pore system. The larger pores with $\tau_4 = 30.3$ ns have a diameter of 2.8 nm if they are spherical. This size is sufficient for accommodating Persantin molecules. The silica gels that are made at the higher pH values have a higher degree of condensation, which prevents a more pronounced shrinking process. This can be clearly followed in the ^{29}Si MAS NMR spectra (Figure 6).

Figure 6 shows the ^{29}Si MAS NMR spectra of the two gels with the highest and lowest synthesis pH values in the series of the single-precursor gels. The condensation degree is higher, as expected, for the gel with the higher synthesis pH (sample 5) and it does not change much when the drug has been released. The sol−gel process at this pH value yields a sufficient degree of cross-linking and network formation to prevent the gel from collapsing. This situation is different for the lower pH value (sample 1), which shows a higher Q^3 content and a higher number of Q^2 units before release. However, Q^3 and Q^2 decrease in favor of more Q^4 sites when the gel has been extracted. This increasing Q^4:Q^3 ratio (from 0.99 to 1.24) is consistent with the suggested shrinking process upon drug release.

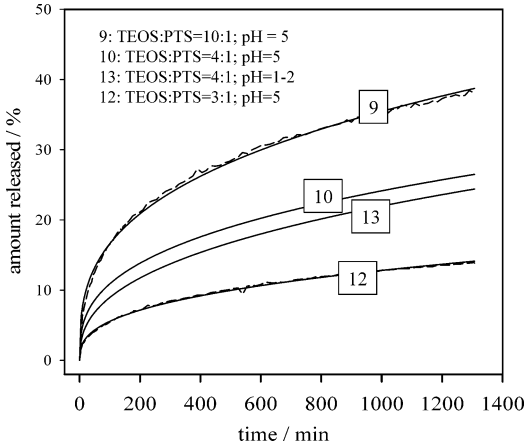

Figure 7. Drug-release experiments of self-assembled hybrid gels with propyl-group functionalization.

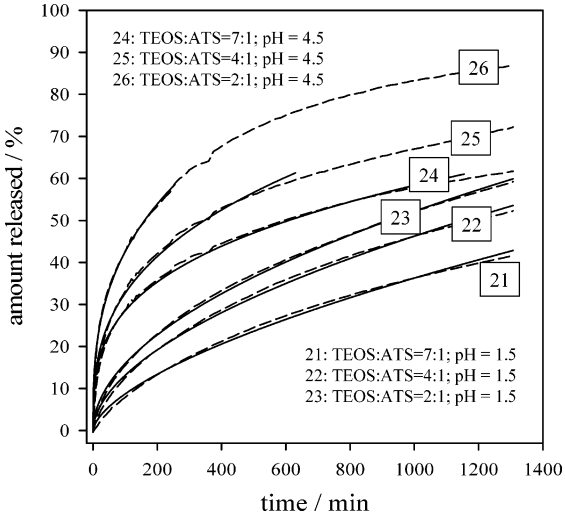

Figure 8. Drug-release experiments of self-assembled hybrid gels with acetoxypropyl-group functionalization.

We conclude from these data that the bimodal pore system in samples with a low synthesis pH is subject to a substantial degree of shrinking when the gel has been extracted. The rigidity and cross-linking of the gel increase with synthesis pH value, and the pore system becomes more robust to the extraction protocol.

The release kinetics (Figure 3) shows a small anomaly with respect to the discussed pore-size trend. The slowest release profile in Figure 3 is observed for the intermediate synthesis pH values of 2.5 and 3.6, whereas the most acidic gel (pH 0.8) shows a faster release despite the complete absence of the larger pores. We interpret this observation by protonation of the silica gel matrix at the smallest pH value of 0.8. The higher pH values of 2.5 and 3.6 are in the range of the isoelectric point of silica. Consequently, a protonated Persantin molecule would be incorporated in a protonated silica matrix at pH 0.8, which leads to a stronger tendency for dissolution than in the pH range of neutral or negatively charged silica. Charge neutrality at low pH can then be rationalized by the inclusion of the desired number of counterions (e.g., Cl^-), resulting in a salt-in-salt inclusion model. This effect will be further discussed below in the context of hybrid gels.

The drug molecule interacts by noncovalent interactions with the sol−gel network during its formation, and the porosity of the gel is clearly different if the drug is not added in the gel-formation step. This shows that the gel network and pore structure are influenced by self-assembly with the drug molecule in the course of matrix genesis. These self-assembled drug-carrier gels clearly show a retarded drug-release kinetics compared to that of impregnated gels in which the drug is encapsulated and/or adsorbed on the surface in a postsynthetic step. Thus, this new approach is a bottom-up manufacturing technique that generates the porosity of the final drug-release vehicle from the drug molecule itself. However, we have been careful to avoid the term "templating", because we cannot rule out that small clusters of several drug molecules act as porogens, especially at weakly acidic pH values.

Hybrid Gels. The release of Persantin from hybrid gels with propyl-group (PTS) functionalization is shown in Figure 7. These gels have been made at two different pH values (1−2 and 5) and with three TEOS:PTS ratios (10:1, 4:1, and 3:1).

Figure 7 clearly shows that a higher level of PTS leads to a decrease in the drug release. On the other hand, the synthesis pH value has a much smaller influence in the release profiles for this sol−gel precursor combination compared to that of the pure TEOS gel. The two gels with the same TEOS:PTS ratio (4:1) and quite different pH values (samples 10 and 13) show rather similar release curves. Hence, the use of PTS causes quite dramatic changes in the release profile, as it inhibits the pH influence.

Propyl functionalization of the carrier gels causes two effects that lead to the observed release characteristics. There is a hydrophobic interaction with Persantin, retarding its dissolution kinetics, and the hydrophobization of the gel also reduces water diffusion in the pores. These hydrophobic effects dominate the release profile over and above the pH influence on pore architecture formation. The same trend can be observed for methyl-functionalized gels. An especially strong retarding effect on the release kinetics is found for carrier gels with phenyl or benzyl groups. These functional groups facilitate $\pi-\pi$ interactions with Persantin, and the drug is strongly encapsulated in these gels (data not shown).

Another precursor used in this study was the acetoxypropylsilyl group (ATS), which exhibits more-hydrophilic properties. The release profiles of gels made at different TEOS:ATS ratios and the two pH values of 4.5 and 1.5 are shown in Figure 8. Here, the pH dependence is again very strong so that the use of organic groups does not suppress a pH dependence. Gels 24−26, which have been made at a higher pH value of 4.5, show a faster initial release than the more acidic materials. The release parameters n and k are listed in Table 2. A striking difference from self-assembled PTS gels is that drug release is accelerated by ATS.

More pH values have been studied, and the release parameters n and k are illustrated in Figure 9. For the pH value of 1.9, the kinetic-release parameters k and n assume a minimum and a maximum value, respectively. This corresponds to release curves with the smallest curvature. The observation that the release curvature increases below

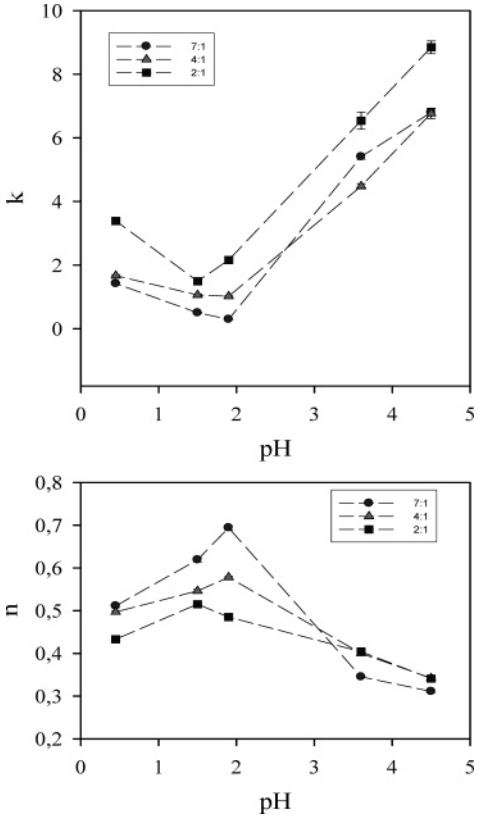

Figure 9. pH dependence of kinetic-release parameters of acetoxypropyl-functionalized hybrid gels; TEOS:ATS ratios are indicated.

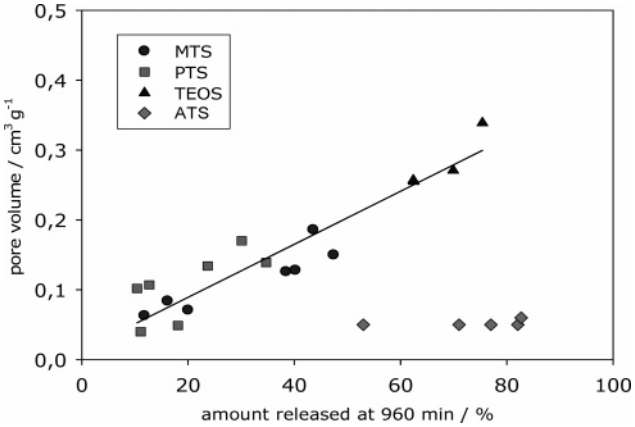

Figure 10. Dependence of free pore volume measured by N_2 adsorption as a function of the released amount of Persantin (at 960 min).

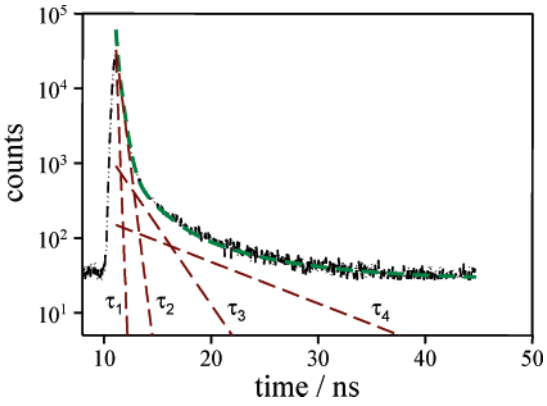

Figure 11. PALS experiment of sample 26.

and above an intermediate acidic pH value was already observed on the pure TEOS gels above (Figure 3).

Persantin is protonated at all pH values of this study, because it has one basic p*K* value of 6.4. The gels that are made near the isoelectric point of silica show the slowest release profile. This is due to the favorable interaction of Persantin in the small pores. At lower pH, the protonated Persantin is surrounded by a protonated matrix (salt inclusion), which favors its dissolution. At higher pH values, larger pores are formed, which also facilitates faster release.

The gels with ATS show a release behavior that differs from that of all the other hybrid gels: an increasing amount of ATS causes a higher level of drug release (Figure 8). PTS and MTS gels as well as other organic functionalities, such as phenyl or benzyl (not shown here), lead to a retarding effect in the drug-dissolution experiment. Therefore, ATS gels seem to be special.

The unusual behavior of the gels with acetoxypropylsilyl (ATS) groups is clearly illustrated in Figure 10. Only gels with a τ_4 lifetime (larger pores) have been included in this figure, because the pores corresponding to τ_3 lifetimes would be too small for N_2 adsorption.

The free pore volume after drug release measured with N_2 adsorption is plotted as a function of the amount released at 960 min. For each gel family (MTS, PTS, TEOS, ATS), different composition and synthesis pH values have been studied. Before drug release, all gels show virtually no accessible pore space. The gels with methyl- or propyl-group functionalization (MTS, PTS) as well as the pure silica gel without organic side groups (TEOS) show a good correlation between the pore volume and the amount of drug released. In contrast, the ATS-functionalized gels do not exhibit an appreciable pore volume (as measured by N_2 adsorption) developing upon drug release.

This special property of the ATS gels, especially the missing N_2 adsorption capacity, compared to the other functionalized gels posed additional questions as to the pore properties of these drug-release systems. This is of particular interest because the ATS gels show a very high level of release. For several reasons, the existence of a separate drug phase prior to the release experiment, for example, on the external surface of a dense gel, can be excluded. Such high levels of the drug in the samples would be easily found as a separate phase. If it were crystalline, X-ray diffraction and melting-point characterizations would clearly identify it, but this was not observed. In addition, electron microprobe analysis of the particle surface did not show any indication of the existence of nitrogen, which would be expected if Persantin were on the surface. Therefore, it is concluded that Persantin must be confined within the gel matrix. There must be another reason the matrix does not adsorb nitrogen after extraction. At this point, PALS became an important tool to further investigate the porosity of the carrier gels to distinguish between two scenarios. Scenario 1 suggests that the ATS gels collapse upon drug release; scenario 2 assumes that a pore volume develops that is, however, not accessible for N_2 adsorption (e.g., by the organic side groups blocking N_2 diffusion at 77 K).

Figure 11 shows the PALS experiment for an extracted ATS gel. The existence of τ_3 and τ_4 decay components shows

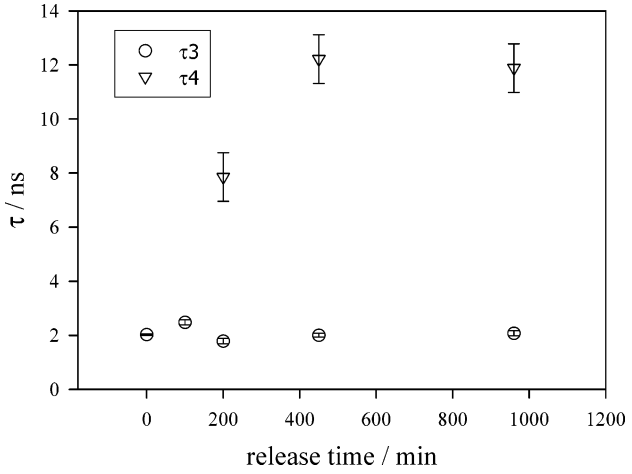

Figure 12. Evolution of pore space detected by PALS for sample 26.

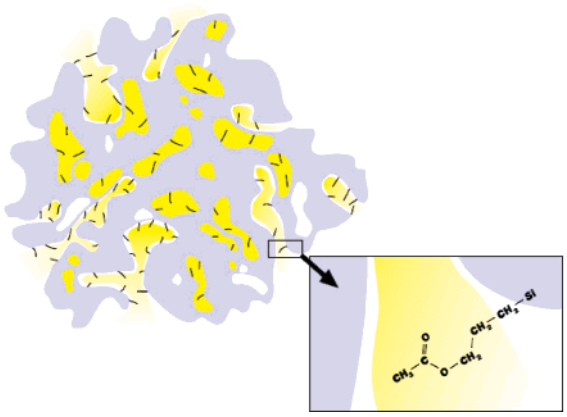

Figure 13. Pore model of ATS gels with acetoxypropyl groups covering the internal and external pore surface and blocking N_2 adsorption at low temperatures.

that pore volume exists in this gel that does not show N_2 adsorption capacity. The advantage PALS has over N_2 adsorption is that positrons can penetrate into the particles to localize in the void volume without the need for channel connections to the external surface.

The increase in the size of the larger pores with release time is shown by the τ_4 component in the PALS experiment (Figure 12). The τ_3 component does not increase, which means the sizes of the smaller voids after extraction are always similar. The intensities, I_3 and I_4, of both components increase with extraction time (not shown), which indicates that the concentration of the pores increases as more drug is extracted.

The PALS experiments on ATS gels unequivocally prove the development of the pore volume upon drug release. Therefore, the fact that no nitrogen is adsorbed for these gels must be explained by N_2 diffusion blockage. It is suggested that this blockage happens because of the organic ATS side groups that possibly form hydrogen bonds, making the chains rather rigid at 77 K, i.e., the temperature at which N_2 adsorption is carried out. ^{1}H MAS NMR investigations clearly show that the motion of organic groups is frozen at around 250 K (not shown), i.e., the groups are more flexible at the release temperature of 334 K. The action of blocking pores toward N_2 adsorption at low temperatures and not blocking pores in the release experiment is a "gating" action, stimulated in this instance by temperature. MTS and PTS are not able to form such hydrogen bonds and do not show a gating effect.

Conclusions

It has been shown that the pharmaceutical drug molecule Persantin can be incorporated in a sol−gel matrix by self-assembly. The release kinetics strongly depends on synthesis parameters (pH, composition of matrix). At highly acidic pH values, the drug is closely surrounded by the gel matrix, leading to the inhibition of the release profile. The use of acetoxypropylsilyl side groups in an inorganic−organic hybrid gel leads to promising release properties. The porosity of the carrier gel shows a bimodal pore-size distribution as measured by positron annihilation lifetime experiments. The smaller pores, characterized by τ_3 in PALS, are not accessible to N_2 adsorption. These smaller pores occur in all gels but dominate in the gel systems that were synthesized in the most acidic pH range. The size of these smaller pores, measured following extraction of the drug, indicates that pore collapse occurs following dissolution.

Generally, the larger pores with a τ_4 component in PALS allow N_2 adsorption with the exception of ATS gels. These larger pores are absent in the most acidic gels. The pores are blocked by the organic ATS side groups for nitrogen adsorption so that virtually no specific surface area can be measured by the standard BET method. Figure 13 illustrates the situation in which the internal pore walls are covered with side groups that are rigid at the N_2 adsorption temperature of 77 K, thus hindering diffusion of the nitrogen molecules. At the release temperature of 334 K, the organic side groups are sufficiently flexible to allow the drug molecule to be extracted. The results suggest that functionalized hybrid gels offer a promising potential for designing drug-release systems for which drug delivery properties can be tailor-made. For pharmaceutical applications, such systems would next have to be investigated by in vivo drug-delivery experiments. The purpose of this work was to explore the synthetic strategies and characterize pore structures that lead to controlled release. In essence, the drug acts as a porogen during the sol−gel synthesis. The self-assembly proceeds during synthesis of the silica gel framework, allowing control over the encapsulation of the drug even at the appreciable loading level of 20% (w/w). This framework then offers the entire range of release rates for standard in vitro conditions by using the synthesis parameters to control the pore-size distribution.

Acknowledgment. We thank the Landesinstitut für den Öffentlichen Gesundheitsdienst NRW for access to the dissolution-rate test equipment. A donation of Persantin by Boehringer Ingelheim (Dr. Peter Sieger) is gratefully acknowledged. This work was produced with the assistance of the Australian Research Council under the ARC Centres of Excellence program.

CM051859O